

# Unstable-particle effective field theory

M. Beneke

*Physik Department T31, James-Frank-Straße 1, Technische Universität München, D-85748 Garching, Germany*

---

## Abstract

Unstable particles are notorious in perturbative quantum field theory for producing singular propagators in scattering amplitudes that require regularization by the finite width. In this review I discuss the construction of an effective field theory for unstable particles, based on the hierarchy of scales between the mass,  $M$ , and the width,  $\Gamma$ , of the unstable particle that allows resonant processes to be systematically expanded in powers of the coupling  $\alpha$  and  $\Gamma/M$ , thereby providing gauge-invariant approximations at every order. I illustrate the method with the next-to-leading order line-shape of a scalar resonance in an abelian gauge-Yukawa model, and results on NLO and dominant NNLO corrections to (resonant and non-resonant) pair production of  $W$ -bosons and top quarks.

**Keywords:** Unstable particles, effective field theory, perturbative quantum field theory, line-shape, top quark,  $W$ -boson

---

## 1. Introduction

The consistency of the Standard Model (SM) of particle physics is tested at high-energy colliders primarily through the production and subsequent decay of unstable particles. New particles, if discovered, are most likely also short-lived. At the current high-energy frontier all known fundamental interactions are perturbatively weak, allowing for very precise theoretical computations in principle. Nevertheless, the application of perturbation theory to processes with unstable particles is not always straightforward.

The very notion of an unstable particle requires clarification. In quantum field theory the fundamental entities are the fields from which the Lagrangian is constructed, but the excitations of the fundamental fields may not correspond to the asymptotic particle states assumed in scattering theory, if they are strongly interacting as is the case for the quarks and gluons of QCD, or unstable with respect to decay into lighter particles. Relevant cases include the electroweak gauge bosons and the top quark, which although all very short-lived, have width over mass ratios of a few percent, larger than the accuracy of precision calculations. Principal questions related to field theories with unstable “particles”

such as their unitarity on the Hilbert space built upon the one-particle states of only stable particles have been answered many years ago [1]. The construction of the unitary  $S$ -matrix is based on certain properties of the exact two-point function of the unstable-particle field. Although a diagrammatic interpretation is assumed, there is no explicit reference to a perturbation expansion in the coupling that renders the particle unstable.

Since exact two-point functions are not at hand, this raises the question of consistent, successive approximations. Ordinary perturbation theory in the Lagrangian coupling  $g$  does not work, since the lowest-order propagator of the unstable particle leads to singularities in scattering amplitudes. A well-known remedy of the singularity is the resummation of self-energy corrections to the propagator, which results in the substitution

$$\frac{1}{p^2 - M^2} \rightarrow \frac{1}{p^2 - M^2 - \Pi(p^2)}. \quad (1)$$

The self-energy has an imaginary part of order  $M^2 g^2 \sim M\Gamma$ , where  $\Gamma$  is the on-shell decay width of the resonance, rendering the propagator large but finite. “Dyson resummation” sums a subset of singular terms of order  $(g^2 M^2 / [p^2 - M^2])^n \sim 1$  (near resonance where  $p^2 \sim M\Gamma$ ) to all orders in the expansion in  $g^2$ . This pro-

cedure leaves open the question of how to identify all terms (and only these) required to achieve a specified accuracy in  $g^2$  and  $\Gamma/M$ . Failure to address this question may lead to a lack of gauge invariance and unitarity of the resummed amplitude, since these properties are guaranteed only order-by-order in perturbation theory, and for the exact amplitude.

Despite the fact that unstable particle fields have no corresponding asymptotic particle states and hence their propagators should never be cut, this point is often ignored in practice and the particle is treated in Feynman diagram and cross section calculations as if it were stable (“narrow-width approximation”). This can be justified when the width is very small, since

$$\frac{M\Gamma}{(p^2 - M^2)^2 + M^2\Gamma^2} \xrightarrow{\Gamma \rightarrow 0} \pi\delta(p^2 - M^2). \quad (2)$$

The limit holds in the distribution sense and is therefore valid only, if the phase-space of the unstable particle is integrated sufficiently inclusively, such that the integration contour in the variable  $p^2$  can be deformed far away from  $M^2$ . This is not always the case. An obvious example is the line-shape, but also distributions may trap the contour near  $M^2$ . A more accurate treatment than (2) is also required, when the desired precision exceeds the leading-order approximation in  $\Gamma/M$ .

Somewhat surprisingly, systematic computational schemes to obtain approximations to scattering processes involving unstable particles in weak coupling expansions are relatively recent. The two, which are general, are the *unstable-particle effective theory* and the *complex mass scheme*.

### 1.1. Unstable-particle effective theory

The singularity of the unstable particle propagator indicates sensitivity to a time scale larger than the Compton wave-length  $1/M$  of the particle, evidently its lifetime  $1/\Gamma$ . The presence of two different scales  $\Gamma \ll M$  lies in the very nature of the problem, since a resonance with  $\Gamma \sim M$  would not be identified as such. The main idea of unstable-particle effective field theory [2, 3] is to exploit this hierarchy of scales in order to systematically organize the calculations in a series in the coupling  $g$ , and  $\Gamma/M$ . The short-distance scale  $M$  is integrated out by performing standard perturbative computations and the full theory is matched to an effective Lagrangian that reproduces the physics at the scale  $\Gamma$ . The effective theory contains a field  $\phi_v$ , which describes a resonance with momentum  $p = Mv + k$ , where only  $k \sim \Gamma$  is fluctuating. The resonant field can interact with other soft fields with momenta of order  $\Gamma$ , but off-shell effects at the scale  $M$  are part of the matching coefficients. The

power-counting of fields and interactions in the effective theory leads to a systematic construction of the expansion in  $\Gamma/M$ .

The expansion of amplitudes in matching calculations is performed around the gauge-invariant location

$$M_\star^2 = M^2 - iM\Gamma \quad (3)$$

of the pole in the complex  $p^2$  plane corresponding to the resonance, where  $M$  is identified with the pole mass, and  $\Gamma$  with the on-shell width. The expansion is similar to the one performed in the “pole” [4, 5] or “double-pole” (in pair production of resonances) [6, 7] approximation. In a certain sense, unstable-particle effective field theory represents the field-theoretic formulation of the diagrammatic pole approximation, and generalizes it to all orders in perturbation theory and beyond the leading power in the  $\Gamma/M$  expansion. A first step in this direction had already been presented in [8].

The effective theory approach is minimal as it identifies precisely the terms required to achieve a specified accuracy in  $g^2$ , and  $\Gamma/M$ , and does not include more. This makes the calculations particularly simple. Furthermore, the operator interpretation allows for the summation of large logarithms of  $\Gamma/M$  through renormalization group equations and anomalous dimensions. There is a draw-back: the details of the effective theory depend on the inclusiveness of the observable and is not valid locally over the entire phase-space, where some portions may involve further soft scales of order  $\Gamma$  in addition to  $(p^2 - M^2)/M$ . Even the prediction of the resonance line-shape requires matching of the resonant (peak) region calculation within the effective theory to the off-resonance region computed with standard perturbation theory.

### 1.2. The complex-mass scheme

The complex-mass scheme is an extension of the standard on-shell renormalization scheme to unstable particles. It defines the complex mass and field renormalization constant from the location and residue of the pole (3) of the unstable-particle propagator. The bare mass  $M_0$  is split into a renormalized mass and counterterm through

$$M_0^2 = M_\star^2 + \delta M_\star^2, \quad (4)$$

and  $\delta M_\star^2$  is part of the interaction Lagrangian and treated as a perturbation. The unstable-particle propagator  $i/(p^2 - M_\star^2)$  is never infinite for physical, real momenta. The complex-mass scheme was discussed already in [9], but it was used for the first time in a full one-loop calculation only in 2005 [10] for the process

$e^+e^- \rightarrow 4 \text{ fermions } (+\gamma)$  at high energies, which receives important contributions from the unstable  $W^+W^-$  intermediate state.

Although the standard rules of perturbation theory and an expansion in the number of loops apply to the complex-mass scheme, a re-ordering and resummation of the  $g^2$  expansion is implicit, since the propagator is of order  $1/(M^2g^2)$  in the resonance region. The assumption is that the complex mass in the propagator captures all terms that need to be resummed which is indeed the case (see also next section). Since the scheme is only a reparameterization of the bare theory, which is not modified, it is obvious that no double counting occurs. Likewise, gauge invariance is assured, since the split (4) is gauge-invariant and the algebraic identities that guarantee gauge invariance are valid in the presence of complex parameters. Unitarity might be a concern, since the unitarity equation involves complex conjugation. However, since the bare theory is unitary, so must be the reparameterized one. What needs to be shown is that the theory with the complex-mass prescription is perturbatively unitary in the sense that unitarity violation in any given order in the loop expansion are of higher order in the expansion parameters (counting  $\Gamma/M \sim g^2$ ). This point was demonstrated explicitly at one-loop for fermion-fermion scattering through a vector-boson resonance [11], and in general in [12].

The complex-mass scheme is conceptually straightforward. It does not require separate treatments of the resonance and off-resonance regions, and can easily be applied to kinematic distributions. Compared to the effective field theory method the scheme does not make use (explicitly) of expansions in  $\Gamma/M$  and hence does not simplify the problem as much as possible in principle. The difficulty of the calculation is equivalent to the corresponding standard loop calculation with the additional complication of loop integrals with complex masses. This is not a practical problem at the one-loop order, making the complex-mass scheme the method of choice for automated next-to-leading order calculations. On the other hand, calculations beyond this order would presently be difficult and the resummation of logarithms  $\ln M/\Gamma$  cannot be performed.

In the following I do not discuss the complex-mass scheme further, but focus on unstable-particle effective theory. I use the line-shape of a resonance to illustrate the framework and the discuss results on pair production of W-bosons and top quarks near threshold which (I believe) benefit particularly from this method.

## 2. Line-shape of an unstable particle

In this section, which follows [2, 3], we consider a toy model that involves a massive scalar field,  $\phi$ , and two fermion fields,  $\psi$ , (the “electron”) are charged under an abelian gauge symmetry, whereas the other fermion,  $\chi$ , (the “neutrino”) is neutral. The model allows for the scalar to decay into an electron-neutrino pair through a Yukawa interaction. The model describes the essential features of the Z-boson line-shape in the SM [13]. Its Lagrangian is

$$\begin{aligned} \mathcal{L} = & (D_\mu \phi)^\dagger D^\mu \phi - \hat{M}^2 \phi^\dagger \phi + \bar{\psi} i \not{D} \psi + \bar{\chi} i \not{\partial} \chi \\ & - \frac{1}{4} F^{\mu\nu} F_{\mu\nu} - \frac{1}{2\xi} (\partial_\mu A^\mu)^2 \\ & + y \phi \bar{\psi} \chi + y^* \phi^\dagger \bar{\chi} \psi - \frac{\lambda}{4} (\phi^\dagger \phi)^2 + \mathcal{L}_{\text{ct}}, \end{aligned} \quad (5)$$

where  $\hat{M}$  denotes the renormalized mass, not necessarily the pole mass  $M$  defined by (4),  $\mathcal{L}_{\text{ct}}$  the counterterm Lagrangian, and  $D_\mu = \partial_\mu - igA_\mu$ . We define  $\alpha_g \equiv g^2/(4\pi)$ ,  $\alpha_y \equiv (yy^*)/(4\pi)$  (at the scale  $\mu$ ) and assume  $\alpha_g \sim \alpha_y \sim \alpha$ , and  $\alpha_\lambda \equiv \lambda/(4\pi) \sim \alpha^2/(4\pi)$ .

The line-shape is the totally inclusive cross section for the process

$$\bar{\nu}(q) + e^-(p) \rightarrow X \quad (6)$$

as a function of  $s \equiv (p+q)^2$ , which can be calculated from the imaginary part of the forward scattering amplitude  $\mathcal{T}(s)$ .<sup>1</sup> In particular, we are interested in the region  $s \approx M^2$ , or more precisely  $s - M^2 \sim M\Gamma \sim \alpha M^2 \ll M^2$ , where we expect an enhancement of the cross section due to the resonant production of the scalar. Defining the dimensionless variable

$$\delta \equiv \frac{s - \hat{M}^2}{\hat{M}^2} \sim \frac{\Gamma}{M}, \quad (7)$$

the cross section far away from the resonance can be expanded in  $g^2$  in the usual manner according to

$$\sigma = g^4 f_1(\delta) + g^6 f_2(\delta) + \dots \quad (8)$$

At every order, the coefficient  $f_n(\delta)$  is a function of the variable  $\delta \sim 1$ . On the other hand, near resonance we may exploit  $\delta \ll 1$  to expand the amplitude in  $\delta$ . At the same time, as  $g^2/\delta \sim 1$  since  $\Gamma \sim Mg^2$ , some terms must be summed to all orders. A systematic approximation

<sup>1</sup>The total cross section of process (6) is not infrared finite for massless electrons due to an initial-state collinear singularity, which has to be absorbed into the electron distribution function. In what follows it is understood that this singularity is subtracted minimally.

to the line-shape in the resonance region therefore takes the form

$$\begin{aligned}\sigma &\sim \sum_n \left(\frac{g^2}{\delta}\right)^n \times \{1 \text{ (LO)}; g^2, \delta \text{ (NLO)}, \dots\} \\ &= h_1(g^2/\delta) + g^2 h_2(g^2/\delta) + \dots\end{aligned}\quad (9)$$

with non-trivial functions  $h_n(g^2/\delta)$  at every order in the reorganized expansion. The effective theory identifies the relevant terms and constructs the expansion (9).

### 2.1. Relevant modes and reduced scattering diagrams

The effective theory is based on the hierarchy of scales  $\Gamma \ll M$ . In a first step we integrate out hard momenta  $k \sim M$ . The effective theory will then not contain any longer dynamical hard modes since their effect is included in the coefficients of the operators. The hard effects are associated with what is usually called factorizable corrections, whereas the effects of the dynamical modes correspond to the non-factorizable corrections [8]. On the level of Feynman diagrams, the hard contribution can be identified directly using the method of regions to separate loop integrals into various contributions [14]. The hard part is obtained by expanding the full-theory integrand in  $\delta$ .

The modes to be described by the effective Lagrangian correspond to kinematically allowed scattering processes with virtualities much smaller than  $M^2$ . Particles with masses above  $M\Gamma$  are no longer present, except for the unstable particle, which by construction is close to mass-shell. To account for this, we write the momentum of the scalar particle as  $P = \hat{M}v + k$ , where the velocity vector  $v$  satisfies  $v^2 = 1$  and the residual momentum  $k$  scales as  $M\delta \sim \Gamma$ . In analogy to heavy-quark effective theory (HQET) we remove the rapid spatial variation  $e^{-i\hat{M}v \cdot x}$  from the  $\phi$  field and define  $\phi_v(x) \equiv e^{i\hat{M}v \cdot x} \mathcal{P}_+ \phi(x)$ , where  $\mathcal{P}_+$  projects onto the positive frequency part to ensure that  $\phi_v$  is a pure destruction field. A field with momentum fluctuations  $k \sim \Gamma$  is called a “soft” field. Thus, for the soft scalar field  $\phi_v$  we have  $P^2 - \hat{M}^2 \sim M^2\delta$ . This remains true if the scalar particle interacts with a soft gauge boson with momentum  $M\delta$ , so the effective Lagrangian should contain soft (s) fields for every massless field of the full theory.

The unstable particle is produced in the scattering of on-shell particles with large energy of order  $M$ . These can remain near mass-shell by radiating further energetic particles in their direction of flight. The effective Lagrangian must therefore also contain hard-collinear (c1) modes with momentum scaling

$$n_+ p \sim M, \quad p_\perp \sim M\delta^{1/2}, \quad n_- p \sim M\delta \quad (10)$$

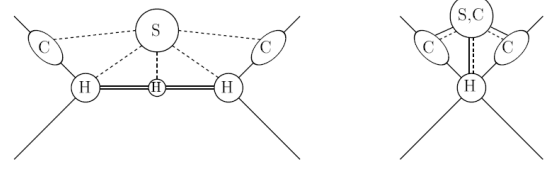


Figure 1: Reduced diagram topologies in  $2 \rightarrow 2$  scattering near resonance. Left: resonant scattering. Right: non-resonant scattering.

for all massless fields of the original Lagrangian. Here  $n_\pm$  are two light-like vectors with  $n_+ \cdot n_- = 2$ ,  $n_-$  is the direction of the electron four-momentum, and  $p_\perp$  is transverse to  $n_-$  and  $n_+$ .<sup>2</sup>

The space-time picture of the kinematically allowed processes is very simple and the corresponding reduced diagram topologies are shown in Figure 1 for the forward-scattering amplitude. The left diagram describes the production of the resonance through a hard process, represented in the effective theory by some local operator  $\mathcal{O}_p^{(k)}$ , and its subsequent propagation over distances of order  $1/\Gamma$ . The resonance (double line) can interact with soft fluctuations. The initial-state electron leg can be dressed with collinear corrections. However, collinear modes cannot be exchanged across the double line, since this would not leave enough energy to produce the scalar near resonance. The process just described is represented in the effective theory by the first line of the master formula

$$\begin{aligned}i\mathcal{T} &= \sum_{k,l} \int d^4x \langle ve | T(i\mathcal{O}_p^{(k)}(0) i\mathcal{O}_p^{(l)}(x)) | ve \rangle \\ &\quad + \sum_k \langle ve | i\mathcal{O}_{\text{nr}}^{(k)}(0) | ve \rangle.\end{aligned}\quad (11)$$

for the forward-scattering amplitude.

The scattering may also occur without the production of the scalar near its mass-shell (right diagram in Figure 1). In the present toy theory this still requires an intermediate scalar line, since the neutrino has only Yukawa interactions. The scalar may be off-shell, because the electron has radiated an energetic (hard or

<sup>2</sup>In the general case several types of collinear modes are required, one for each direction defined by energetic particles in the initial and final state. For the inclusive line-shape we calculate the forward-scattering amplitude, so no direction is distinguished in the final state. We then need two sets of collinear modes, one for the direction of the incoming electron, labelled by “c1” (or often simply “c”), the other for the direction of the incoming neutrino (labelled “c2”). Since the neutrino is electrically neutral, the collinear fields  $\psi_{c2}$ ,  $A_{c2}$  and  $\chi_{c1}$  appear only in highly suppressed terms, so we can ignore them here.

collinear) photon before it hits the neutrino. In this case the invariant mass of the colliding electron-neutrino system is of order  $M^2$  but not near  $M^2$ , producing a non-resonant scalar. In the effective theory this process is represented by a local four-fermion operator  $\mathcal{O}_{\text{nr}}^{(k)}$ , without  $\phi_v$  fields. In general, non-resonant scattering includes all “background processes”, which produce one of the final states under consideration. This topology does not involve a resonant heavy scalar, and both soft and collinear fields can be exchanged across the diagram. The matrix elements in (11) are understood to be evaluated with the effective Lagrangian.

## 2.2. Construction of the effective Lagrangian

We divide the effective Lagrangian into three parts. Roughly speaking, the first,  $\mathcal{L}_{\text{HSET}}$ , describes the heavy scalar field near mass-shell and its interaction with the gauge field. The second part,  $\mathcal{L}_{\pm}$ , describes energetic fermions and their interactions with the gauge field. Finally, the third part,  $\mathcal{L}_{\text{int}}$  contains the local operators  $\mathcal{O}_p^{(k)}$  and  $\mathcal{O}_{\text{nr}}^{(k)}$  responsible for the production of the resonance and off-shell processes. In the following, we write down all terms needed for a next-to-leading order (NLO) calculation of the line-shape.

The soft Lagrangian  $\mathcal{L}_{\text{HSET}}$  is an extension of the HQET Lagrangian [15] to a (here scalar) particle whose mass-shell is defined by the complex pole location (4). The residual mass term which is usually set to zero in HQET by choosing  $M$  to be the pole mass of the heavy quark, is now necessarily non-vanishing and complex. The relevant terms are

$$\begin{aligned} \mathcal{L}_{\text{HSET}} = & 2\hat{M}\phi_v^\dagger \left( i v \cdot D_s - \frac{\Delta^{(1)}}{2} \right) \phi_v \\ & + 2\hat{M}\phi_v^\dagger \left( \frac{(iD_{s,\perp})^2}{2\hat{M}} + \frac{[\Delta^{(1)}]^2}{8\hat{M}} - \frac{\Delta^{(2)}}{2} \right) \phi_v \\ & - \frac{1}{4} F_{s\mu\nu} F_s^{\mu\nu} + \bar{\psi}_s i \not{D}_s \psi_s + \bar{\chi}_s i \not{\partial} \chi_s, \end{aligned} \quad (12)$$

where  $\psi_s$  ( $\chi_s$ ) denotes the soft electron (neutrino) field and the covariant derivative  $D_s \equiv \partial - igA_s$  includes the soft photon field. Furthermore,  $a_\tau^\mu \equiv a^\mu - (v \cdot a) v^\mu$  for any vector. The only non-trivial short-distance matching coefficients in this expression are the quantities  $\Delta^{(i)}$  to be defined below.

The bilinear terms in the soft scalar field  $\phi_v$  are determined by the requirement that  $\mathcal{L}_{\text{HSET}}$  reproduces the two-point function of the scalar in the full theory close to resonance. Denoting the complex pole of the propagator by  $M_\star^2$  and the residue at the pole by  $R_\phi$ , the prop-

agator near resonance can be written as

$$\frac{i R_\phi}{P^2 - M_\star^2} = \frac{i R_\phi}{2\hat{M}v \cdot k + k^2 - (M_\star^2 - \hat{M}^2)}. \quad (13)$$

We now define the matching coefficient  $\Delta \equiv (M_\star^2 - \hat{M}^2)/\hat{M}$ . There are two solutions to  $P^2 = M_\star^2$ , one of which is irrelevant since it scales as  $v \cdot k \sim \hat{M}$ . For the other we find

$$\begin{aligned} v \cdot k &= -\hat{M} + \sqrt{\hat{M}^2 + \hat{M}\Delta - k_\perp^2} \\ &= \frac{\Delta}{2} - \frac{\Delta^2 + 4k_\perp^2}{8\hat{M}} + \mathcal{O}(\delta^3), \end{aligned} \quad (14)$$

where we expanded in  $\delta$  in the second line, using  $\Delta \sim k_\perp \sim M\delta$ . Expanding  $\Delta = \sum_{i=1} \Delta^{(i)}$  into terms of order  $g^{2i}$ , we deduce the bilinear terms in (12) from the dispersion relation (14). Gauge invariance of the effective Lagrangian implies that the leading soft-photon interactions can be obtained from the bilinear terms by replacing  $\partial \rightarrow D_s$ . The gauge invariance of the matching coefficient follows from the invariance of the unstable-particle pole  $M_\star$ .

In the underlying theory the full renormalized propagator of the unstable particle is given by  $i(s - \hat{M}^2 - \Pi(s))^{-1}$ , where  $-i\Pi(s)$  corresponds to the amputated 1PI graphs including counterterms. Comparing this to (13) and expanding  $\Pi(s)$  around  $\hat{M}^2$  and in the number of loops in the form  $\Pi(s) = \hat{M}^2 \sum_{k,l} \delta^l \Pi^{(k,l)}$ , where it is understood that  $\Pi^{(k,l)} \sim g^{2k}$ , we obtain

$$\Delta = \hat{M} \Pi^{(1,0)} + \hat{M} (\Pi^{(2,0)} + \Pi^{(1,1)} \Pi^{(1,0)}) + \dots \quad (15)$$

$\Pi^{(1,0)}$  and  $\Pi^{(2,0)} + \Pi^{(1,1)} \Pi^{(1,0)}$  (but not  $\Pi^{(2,0)}$  and  $\Pi^{(1,1)}$  separately) are infrared-finite, which justifies the interpretation of  $\Delta$  as a short-distance coefficient. Explicit results for  $\Delta^{(1)}$  and  $\Delta^{(2)}$  in the  $\overline{\text{MS}}$  and pole renormalization scheme can be found in [3]. Here we only note that in the pole scheme ( $\hat{M} \equiv M$ ), we have  $\Delta = -i\Gamma$ , in which case the residual “mass” is purely imaginary and coincides with the on-shell width.

Each term in  $\mathcal{L}_{\text{HSET}}$  can be assigned a scaling power in  $\delta$ . Since  $D_s \sim k \sim \Gamma \sim M\delta$  and  $\Delta^{(1)} \sim Mg^2 \sim M\delta$ , both terms in the first line of (12) are of equal size and leading terms. The unstable-particle propagator is therefore

$$\frac{i}{2\hat{M}(v \cdot k - \Delta^{(1)}/2)}, \quad (16)$$

which corresponds to a fixed-width prescription. The linearity of the propagator in the (residual) momentum makes calculations in the effective theory particularly

simple. The fact that only  $\Delta^{(1)}$  appears in the leading-order Lagrangian proves that only the two-point function in the original theory needs to be resummed by including the one-loop self-energy into the unperturbed Lagrangian. No higher-point functions require resummation, which is intuitively obvious, since the origin of the long-distance scale is associated with a single-particle effect, the life-time of the resonance.

In momentum space the propagator (16) of the  $\phi_v$  field scales as  $1/\delta$ . Hence, because  $\int d^4k$  counts as  $\delta^4$ , the soft scalar field  $\phi_v(x)$  scales as  $\delta^{3/2}$ . It follows that the terms in the second line of (12) scale as  $\delta^5$ . Being suppressed by one power in  $\delta$  or  $g^2$  relative to the first line, they must be included only in a calculation of the line-shape with NLO precision. Finally, since  $A_s^\mu$  scales as  $\delta$  and the soft fermion fields scale as  $\delta^{3/2}$ , the terms in the last line of (12) scale as  $\delta^4$  and represent leading interactions among the soft, massless modes. By adding further terms the Lagrangian can be improved to any accuracy desired.

Next, we turn to the construction of the effective Lagrangian,  $\mathcal{L}_\pm$ , associated with the energetic fermions. The interactions of collinear modes with themselves and with soft modes are described within soft-collinear effective theory (SCET) [16, 17, 18, 19]. The coupling of collinear modes to the scalar field  $\phi_v$ , and among collinear fields with different directions produces off-shell fluctuations, which are not part of the effective Lagrangian. The momenta associated with generic collinear fields  $\psi_{c1}$  and  $\bar{\chi}_{c2}$  do not add up to a momentum of the form  $P = Mv + k$ . This kinematic constraint is implemented by adding the production and non-resonant operators,  $\mathcal{O}_p^{(k)}$  and  $\mathcal{O}_{nr}^{(k)}$ , respectively, as external “sources” for the specific process. The line-shape is then given by the correlation function (11).

Alternatively, the dynamical hard-collinear modes can be integrated out in a second matching step, in which the collinear functions (labelled “C” in Figure 1) appear as matching coefficients of (non-local) operators. The new effective Lagrangian contains an “external-collinear” electron mode with momentum  $\hat{M}n_-/2 + k$ , which describes the remaining soft fluctuations  $k \sim \delta$  around the fixed large component. Similar to the resonance field, we extract the large component and define  $\psi_{n_-}(x) \equiv e^{i\hat{M}/2(n_-x)} \mathcal{P}_+ \psi_{c1}(x)$ , where  $\mathcal{P}_+$  projects on the positive frequency part of  $\psi_{c1}$ . Adding the corresponding field with  $n_-$  and  $n_+$  exchanged for the neutrino, the soft interactions of the external-collinear field are given by

$$\mathcal{L}_\pm = \bar{\psi}_n i n_- D_s \frac{\not{n}_+}{2} \psi_{n_-} + \bar{\chi}_{n_+} i n_+ \partial \frac{\not{n}_-}{2} \chi_{n_+}. \quad (17)$$

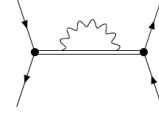


Figure 2: Scalar self-energy correction to the forward-scattering amplitude.

at leading power.

With the external-collinear modes we can implement the production and non-resonant sources as interaction terms in  $\mathcal{L}_{\text{int}}$ . At NLO the relevant terms read

$$\begin{aligned} \mathcal{L}_{\text{int}} = & C y \phi_v \bar{\psi}_{n_-} \chi_{n_+} + C y^* \phi_v^\dagger \bar{\chi}_{n_+} \psi_{n_-} \\ & + D \frac{yy^*}{\hat{M}^2} (\bar{\psi}_{n_-} \chi_{n_+}) (\bar{\chi}_{n_+} \psi_{n_-}), \end{aligned} \quad (18)$$

where  $C = 1 + \mathcal{O}(\alpha)$  and  $D$  are the matching coefficients. The two lines correspond to the two reduced diagram topologies in Figure 1. We note that the effective Lagrangian is not manifestly hermitian, since it describes the decay of the scalar. Nevertheless, it generates a unitary time evolution, since it reproduces by construction the unitary underlying theory to the specified order in the expansion in  $\delta$ .

The external fields scale as  $\delta^{3/2}$ . Thus, an insertion of a  $\phi\psi\chi$  operator results in  $\int d^4x \phi_v \bar{\psi}_{n_-} \chi_{n_+} \sim \delta^{1/2}$ . The forward-scattering amplitude requires two insertions of this operator. Accounting for the scaling of the external state  $\langle \bar{\nu} e^- | \sim \delta^{-1}$ , we find  $\mathcal{T}^{(0)} \sim g^2/\delta$  for the amplitude at leading order, which is the expected result. The four-fermion operator is suppressed in  $\delta$  and results in a contribution of order  $g^2$  to  $\mathcal{T}$ . Thus, to compute the NLO correction  $\mathcal{T}^{(1)}$  we need  $C^{(1)}$ , the  $\mathcal{O}(g^2)$  contribution to the matching coefficient  $C$ , while  $D$  is only needed at tree level. The matching coefficients are obtained from the hard contributions to the corresponding on-shell three- and four-point functions in the full theory. I refer to [3] for the precise matching equation as well as the explicit results.

### 2.3. Example diagram

It is instructive to discuss how the self-energy correction to the intermediate scalar in the full theory, see Figure 2, is represented in the effective description. We first separate the hard and soft contributions the one-loop self-energy,  $\Pi(s) = \Pi_h(s) + \Pi_s(s)$ , and then expand the hard part  $\Pi_h(s) = \hat{M}^2 \sum_l \delta^l \Pi^{(1,l)}$ . The soft part is reproduced by the effective theory self-energy. The first term  $\Pi^{(1,0)}$  in the hard expansion is gauge-invariant and contributes to  $\Delta^{(1)}$  as discussed before. This term is already relevant to the leading-order line-shape. The next

term  $\Pi^{(1,1)}$  cancels one of the adjacent scalar propagators, such that the self-energy correction merges with the local production vertex.  $\Pi^{(1,1)}$  is gauge-dependent. The gauge dependence cancels with the vertex diagram to produce a gauge-independent NLO hard-matching coefficient  $C^{(1)}$ . Continuing in this way, we find that  $\Pi^{(1,2)}$  contributes to the one-loop matching coefficient  $D^{(1)}$  of the four-fermion operator  $(\bar{\psi}_{n-}\chi_{n+})(\bar{\chi}_{n+}\psi_{n-})$ , because the scalar propagators to the left and right are both cancelled. The contribution is again required to obtain a gauge-invariant one-loop matching coefficient [3], though it is already a NNLO term for the line-shape.

This example illustrates the power of the effective field theory method. It automatically breaks a diagram into different pieces and organizes them into gauge-invariant objects. The power-counting associated with the Lagrangian allows one to identify the terms relevant for a specified accuracy before any explicit calculation needs to be performed.

#### 2.4. Line-shape at next-to-leading order

Our goal is to carry out this programme for the forward-scattering amplitude  $\mathcal{T}^{(0)} + \mathcal{T}^{(1)}$  at NLO, where  $\mathcal{T}^{(0)}$  sums up all terms that scale as  $(g^2/\delta)^n \sim 1$  and  $\mathcal{T}^{(1)}$  contains all terms that are suppressed by an additional power of  $g^2$  or  $\delta$ . At leading order there is only one diagram, involving two three-point vertices and one resonant scalar propagator. We get

$$i\mathcal{T}^{(0)} = \frac{-iyy^*}{2\hat{M}\mathcal{D}} [\bar{u}(p)v(q)] [\bar{v}(q)u(p)], \quad (19)$$

where we defined  $\mathcal{D} \equiv \sqrt{s} - \hat{M} - \Delta^{(1)}/2$ . The inclusive line-shape is related to  $\mathcal{T}^{(0)}$  by  $\sigma = \text{Im} \mathcal{T}^{(0)}/s$  through the optical theorem. The above expression gives a Breit-Wigner distribution in  $\sqrt{s}$ .

In the effective theory there are three classes of diagrams that contribute to  $\mathcal{T}^{(1)}$ , corresponding to hard, hard-collinear and soft contributions. The hard-collinear corrections to the external lines lead to scaleless integrals and vanish. The hard corrections consist of a propagator insertion  $[\Delta^{(1)}]^2/4 - \hat{M}\Delta^{(2)}$ , a production vertex insertion  $C^{(1)}$ , and a four-point vertex diagram due to the  $(\bar{\psi}\chi)(\bar{\chi}\psi)$  operator in  $\mathcal{L}_{\text{int}}$ , as shown in the upper diagrams of Figure 3. The sum of these diagrams reads

$$i\mathcal{T}_h^{(1)} = i\mathcal{T}^{(0)} \times \left[ 2C^{(1)} - \frac{[\Delta^{(1)}]^2}{8\hat{M}} + \frac{\Delta^{(2)}}{2\mathcal{D}} - \frac{\mathcal{D}}{2\hat{M}} \right]. \quad (20)$$

The soft-photon one-loop corrections (lower set of diagrams in Figure 3) computed in the effective theory

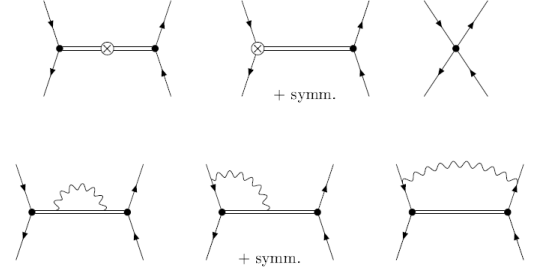


Figure 3: Hard (upper) and soft (lower diagrams) contributions to  $\mathcal{T}^{(1)}$ .

result in

$$i\mathcal{T}_s^{(1)} = i\mathcal{T}^{(0)} \times \frac{g^2}{(4\pi)^2} \left[ 4L^2 - 4L + \frac{5\pi^2}{6} \right] \quad (21)$$

with  $L = \ln(-2\mathcal{D}/\mu)$ . The partonic line-shape is obtained after subtracting the initial-state collinear singularity and taking the imaginary part. The partonic line-shape must then be convoluted with the electron distribution function.

We note the simplicity of the result, which is a consequence of the fact that the complete calculation is broken into separate single-scale calculations by factorizing the hard and soft regions. The NLO correction leads to a distortion of the line-shape relative to the Breit-Wigner form, which in non-inclusive situations can depend on the final state. Fitting a measured line-shape to the Breit-Wigner form rather than the true shape predicted by theoretical calculations leads to errors in mass determinations. In the present toy model, choosing the pole mass  $M = 100$  GeV (such that the  $\overline{\text{MS}}$  mass is  $\hat{M} = 98.8$  GeV at LO and  $\hat{M} = 99.1$  GeV at NLO) and couplings  $g^2/(4\pi) = |y|^2/(4\pi) = 0.1$  to mimic the parameters of electroweak gauge bosons, the error would be of order 100 MeV.

Figure 4 shows the leading-order partonic line-shape in the effective theory and the tree-level (order  $\alpha^2$ ) cross section off resonance in the full theory. The two results agree in an intermediate region where both calculations are valid. This allows to obtain a consistent LO result for all values of  $\sqrt{s}$ . The figure also shows the NLO line-shape for the numerical values given above. In order to obtain an improved NLO result in the entire region of  $\sqrt{s}$ , the NLO line-shape would have to be matched to the NLO off-resonance cross section in the full theory.

The method discussed here makes NNLO line-shape calculations in  $2 \rightarrow 2$  scattering possible with present techniques. An outline of such a calculation has been

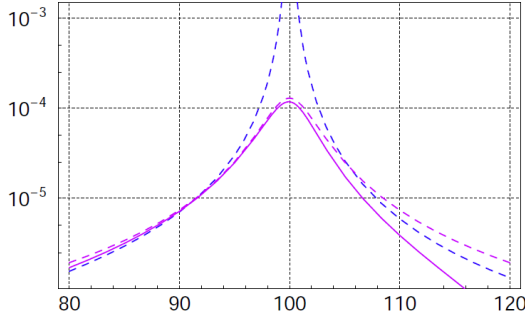


Figure 4: The line-shape (in  $\text{GeV}^{-2}$ ) in the effective theory at LO (light grey/magenta dashed) and NLO (light grey/magenta) and the LO cross section off resonance in the full theory (dark grey/blue dashed) as a function of the centre-of-mass energy (in GeV). Figure from [2].

given in [3], though no complete calculation has been performed to date.

### 3. Pair production near threshold

I reviewed in some detail the case of the line-shape, since it serves well to illustrate the general framework of unstable-particle effective theory. However, some of the more interesting results concern pair production of unstable particles, specifically the  $W$  bosons and top quarks, near threshold. In  $e^+e^-$  collisions very precise measurement of the masses of these particles can be obtained from a threshold scan.

The threshold dynamics is determined by the interplay of the strength of the electromagnetic ( $W$  bosons) or colour (top quarks) Coulomb force and the size of the decay width of the particle. The small parameters are

$$\delta \equiv \frac{\Gamma}{M}, \quad v^2 \equiv (\sqrt{s} - [2M + i\Gamma])/M, \quad (22)$$

and the coupling  $\alpha = g^2/(4\pi)$ . For  $W$  bosons,  $\Gamma_W \sim M_W \alpha_{\text{EW}}$  and therefore the effective strength of the Coulomb force is  $\alpha_{\text{em}}/v \sim \sqrt{\delta} \ll 1$ . This leads to an enhancement, but the Coulomb force is never  $\mathcal{O}(1)$ , and no resummation is needed [20]. The rapid decay of the  $W$  boson prevents the formation of any visible  $W^+W^-$  resonance. The situation is different for top quarks, since the

Coulomb force is generated by QCD, while the decay still occurs through the electroweak interaction. Counting  $\alpha_s \sim \alpha_{\text{EW}}^2$ , we now find  $\alpha_s/v \sim 1$ . Diagrammatically, ladder diagrams that contain these enhanced terms must be summed to all orders in perturbation theory, which generates toponium bound-states in the spectral functions. Since the characteristic energy near threshold  $E \sim Mv^2$  is of order  $\Gamma$ , the bound-states appear as broad resonances, of which only the first one leaves a distinctive feature in the  $t\bar{t}$  cross section [21, 22].

In the following I review results for  $W$  and top pair production near threshold obtained within the effective field theory approach, leaving out all the technical details that can be found in the original papers.

#### 3.1. $W$ bosons

This subsection summarizes results from [23, 24]. We consider the process  $e^-e^+ \rightarrow \mu^-\bar{\nu}_\mu u\bar{d} X$  with centre-of-mass energy  $\sqrt{s} = 160 \dots 170 \text{ GeV}$ , where it is dominated by a  $W^+W^-$  intermediate state near threshold with subsequent semi-hadronic decay. The inclusive cross section is extracted from specific cuts of the forward amplitude

$$\hat{\sigma} = \frac{1}{s} \text{Im} \mathcal{A}(e^-e^+ \rightarrow e^-e^+)_{\mu^-\bar{\nu}_\mu u\bar{d}}, \quad (23)$$

which also includes diagrams with only a single internal  $W$  line. We perform a “QCD-style” calculation of the “partonic” cross section  $\hat{\sigma}$  with massless electrons in the  $\overline{\text{MS}}$  scheme, and convolute it with the  $\overline{\text{MS}}$  electron distribution function:

$$\sigma(s) = \int_0^1 dx_1 dx_2 f_{e/e}(x_1) f_{e/e}(x_2) \hat{\sigma}(x_1 x_2 s). \quad (24)$$

The  $\overline{\text{MS}}$  electron distribution function depends on  $m_e$ , but not on  $\sqrt{s}$ ,  $M$ ,  $\Gamma$ .

In the effective field theory (EFT) the  $W$  bosons are described by two non-relativistic three-vector fields  $\Omega_a^i$ , where  $a = \pm$  refers to the charge of the  $W$ . The HSET Lagrangian relevant to a single (scalar) unstable particle is replaced by the PNRQED Lagrangian [25], generalized to the case of an unstable vector particle. The relevant terms are

$$\mathcal{L}_{\text{PNRQED}} = \sum_{a=\mp} \left[ \Omega_a^{\dagger i} \left( iD_s^0 + \frac{\vec{\partial}^2}{2M_W} - \frac{\Delta}{2} \right) \Omega_a^i + \Omega_a^{\dagger i} \frac{(\vec{\partial}^2 - M_W \Delta)^2}{8M_W^3} \Omega_a^i \right] + \int d^3\vec{r} [\Omega_-^{\dagger i} \Omega_-^i](x + \vec{r}) \left( -\frac{\alpha_{\text{em}}}{r} \right) [\Omega_+^{\dagger j} \Omega_+^j](x). \quad (25)$$



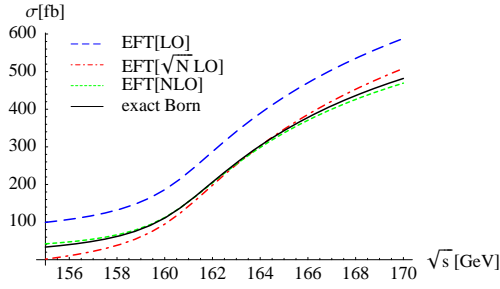


Figure 5: Successive EFT approximations: LO (long-dashed/blue),  $N^{1/2}$ LO (dash-dotted/red) and NLO (short-dashed/green). The solid/black curve is the full Born result computed with Whizard/CompHep. The  $N^{3/2}$ LO EFT approximation is indistinguishable from the full Born result on the scale of this plot. Figure from [23].

The master formula for the forward amplitude  $\mathcal{A}$  coincides with (11), but the production and non-resonant operators are now of the form

$$\mathcal{O}_p^{(k)} = C_p^{(k)} \left( \bar{e}_{c_2, L/R} \gamma^{[i} n^{j]} e_{c_1, L/R} \right) \left( \Omega_-^{\dagger i} \Omega_+^{\dagger j} \right), \quad (26)$$

$$\mathcal{O}_{\text{nr}}^{(k)} = C_{\text{nr}}^{(k)} (\bar{e}_{c_1} \Gamma_1 e_{c_2}) (\bar{e}_{c_2} \Gamma_2 e_{c_1}), \quad (27)$$

with  $\Gamma_1, \Gamma_2$  Dirac matrices,  $a^{[i} b^{j]} \equiv a^i b^j + a^j b^i$ , and  $\vec{n}$  the unit-vector in the direction of the incoming electron three-momentum.

Due to the  $1/\nu$  enhancement of electromagnetic Coulomb exchange, the systematic expansion of  $\mathcal{A}$  goes in powers of  $\sqrt{\delta}$ . Also, the non-resonant term appears as such a “ $N^{1/2}$ LO” correction, since the leading imaginary parts of  $C_{\text{nr}}^{(k)}$  are proportional to  $\alpha^3$ , while  $\mathcal{A} \sim \alpha^2 \sqrt{\delta}$ .<sup>3</sup>

The EFT constructs an expansion in  $\Gamma/M$  and  $(\sqrt{s} - 2M)/M$  of the full theory Born cross section. Before turning to radiative corrections it is instructive to compare successive terms in this expansion to the full Born result computed numerically (using Whizard [26] and CompHep [27]). This is shown in Figure 5. The LO non-relativistic approximation overestimates the true result. The  $N^{1/2}$ LO non-resonant correction yields a (nearly) constant, negative term and provides already good agreement close to the nominal threshold at  $\sqrt{s} \approx 161$  GeV. To extend the approximation in a wider region around the threshold, it is necessary to include all terms up to  $N^{3/2}$ LO.

<sup>3</sup>The factor  $\sqrt{\delta}$  arises from the leading-order EFT matrix element and corresponds to the phase-space suppression near threshold.

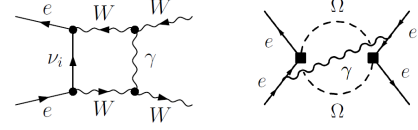


Figure 6: One-loop diagram for the hard-matching coefficient (left) and a soft NLO contribution to the forward-scattering amplitude in the effective theory (right).

While constructing an expansion of the Born cross section when an exact, numerical result is readily available, appears as an unnecessary complication, the computation of the NLO radiative correction in unstable-particle effective theory [23] is remarkable simple compared to the corresponding calculation in the complex-mass scheme [10, 28]. The most complicated part is the computation of the NLO matching coefficient of the operator (26), which, however, is a standard one-loop calculation. A representative diagram is shown in Figure 6 left. The diagram on the right displays a soft, “non-factorizable” NLO correction to the two-point function of production operators in (11), and results again in a simple expression, similar to (21). A comparison with the complex-mass scheme calculation and the double-pole approximation (DPA), including QCD corrections and initial-state radiation is given in the following table.<sup>4</sup> The numerical difference of 1% between the EFT and full ee4f results is presumably in part due to the  $N^{3/2}$ LO correction associated with the NLO matching coefficient of  $\mathcal{O}_{\text{nr}}^{(k)}$ , which is implicitly contained in the NLO full ee4f calculation.

	$\sigma(e^- e^+ \rightarrow \mu^- \bar{\nu}_\mu u \bar{d} X)(\text{fb})$			
$\sqrt{s} [\text{GeV}]$	Born (SM)	EFT	full ee4f	DPA
161	107.06(4)	117.38(4)	118.77(8)	115.48(7)
170	381.0(2)	399.9(2)	404.5(2)	401.8(2)

We can now estimate the theoretical uncertainty in the  $W$  mass determination from a threshold scan. Figure 7 shows  $\kappa = \sigma(s, M_W + \delta M_W)/\sigma(s, M_W)$  for  $M_W = 80.377$  GeV and different values of  $\delta M_W$  as function of the cms energy. The relative change in the cross section is shown as dashed lines for  $\delta M_W = \pm 15, \pm 30, \pm 45$  MeV. The shape of these curves shows that the sensitivity of the cross section to the  $W$  mass is largest around the nominal threshold  $\sqrt{s} \approx 161$  GeV, as expected, and rapidly decreases for larger  $\sqrt{s}$ . (The loss in sensitivity is partially compensated by a larger cross section, implying smaller statistical errors of the anticipated experimental data.) The shaded areas provide an

<sup>4</sup>The “full ee4f” column refers to the erratum of [28].

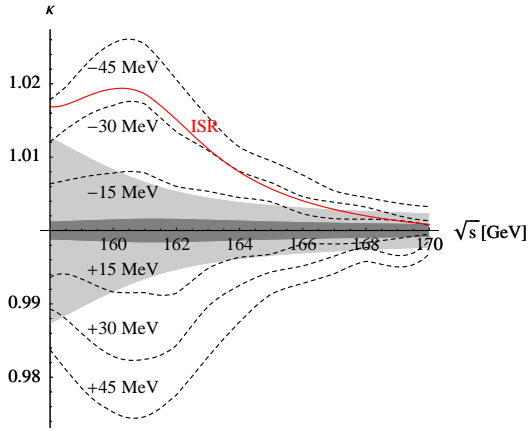


Figure 7:  $W$ -mass dependence of the total cross section. All the cross sections are normalized to  $\sigma(s, M_W = 80.377 \text{ GeV})$ . See text for explanations. Figure from [23].

estimate of the uncertainty from uncalculated  $N^{3/2}\text{LO}$  terms. The inner band is associated with the interference of single Coulomb exchange with one-loop hard or soft corrections, which are genuine NNLO corrections in other schemes. The outer band accounts for the non-resonant term already mentioned above. Finally, the line marked “ISR” estimates ambiguities in the implementation of initial-state radiation. This represents the largest current uncertainty. In order to obtain a competitive determination of  $M_W$ , one eventually needs a more accurate computation of the electron distribution function.

Since this is not a fundamental problem and since the full theory NLO  $ee4f$  calculation is available, the accuracy of the theoretical prediction is limited by the  $N^{3/2}\text{LO}$  terms in the  $\delta$  expansion, which correspond to two-loop corrections (in the complex-mass scheme). Some of the diagrams together with their EFT representation are shown in Figure 8. These consist of mixed hard-Coulomb corrections (first column), interference of Coulomb exchange with soft and collinear radiative corrections (2nd and 3rd column, respectively), and a correction to the electromagnetic Coulomb potential itself. These genuine higher-order corrections have been computed [24] and were found to be below 0.5%, leading to shifts of  $W$  mass of less than 5 MeV.

Up to now, we considered the total cross section for the flavour-specific final state  $\mu^- \bar{\nu}_\mu u \bar{d} X$ . Since experimentally certain cuts must be applied, it would be desirable to compute directly the cut cross section in the EFT. A framework to implement arbitrary cuts while main-

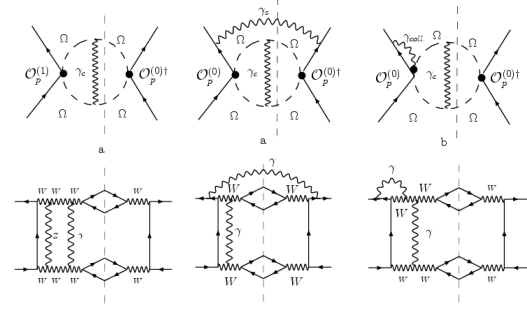


Figure 8: Some NNLO diagrams that count as  $N^{3/2}\text{LO}$  in the  $\delta$  expansion and their EFT representation (upper line).

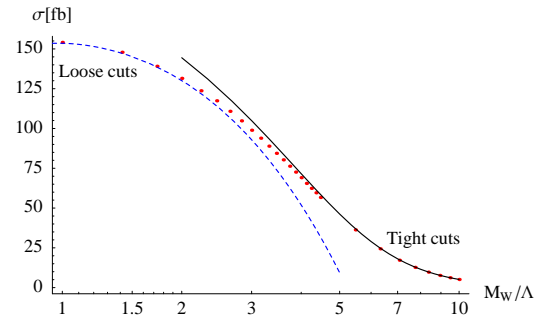


Figure 9: Comparison of the Born cross section in the full SM at  $\sqrt{s} = 161 \text{ GeV}$  computed with WHIZARD (red dots) with the effective-theory result for the loose-cut implementation (dashed blue curve) and the tight-cut implementation (solid black curve). Figure from [24].

taining an expansion in the power-counting parameter  $\delta$  is not available and probably difficult to achieve. The specific case of invariant-mass cuts  $|M_{f_i f_j}^2 - M_W^2| < \Lambda^2$  on the  $W$ -decay products has been considered in [24]. The implementation depends on how  $\Lambda$  scales with the parameter  $\delta$ . For loose cuts,  $\Lambda \sim M_W$ . Since by assumption the virtualities in the EFT are at most of order  $M\Gamma \sim M\delta$ , the loose cut does not affect the EFT diagrams. However, the hard-matching coefficients are modified and acquire a dependence on  $\Lambda$  in addition to the other short-distance scales. The situation is reversed for tight cuts with  $\Lambda \sim M\Gamma \sim M\sqrt{\delta}$ . The tight cut cuts into the (approximate) Breit-Wigner distribution of the single- $W$  invariant mass distribution and therefore must be applied to the calculation of the EFT loop integrals. On the other hand, it eliminates off-shell contributions, and hence the short-distance coefficient  $C_{\text{nr}}^{(k)}$  of the non-resonant four-electron operator (27) vanishes. Figure 9 shows good agreement of the effective-theory calculation of the cut Born cross section with the numerical result from WHIZARD in the regions where the respective loose/tight-cut counting rule is appropriate.

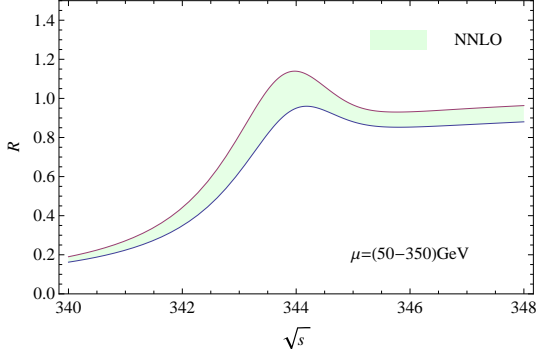


Figure 10: Top quark pair production cross section near threshold, normalized to  $4\pi\alpha_{\text{em}}^2/(3s)$  at NNLO in non-relativistic, resummed perturbation theory in the PS mass scheme [29]. The width of the band reflects the theoretical uncertainty estimated from scale variation in the indicated range.  $m_{t,\text{PS}}(20 \text{ GeV}) = 171.5 \text{ GeV}$ ,  $\Gamma_t = 1.33 \text{ GeV}$ .

### 3.2. Top quarks

The strong Coulomb attraction of the coloured top quarks, when their relative velocity is small near threshold, requires the resummation of certain QCD corrections to all orders in perturbation theory. A systematic formalism employs a sequence of matching steps to define hard matching coefficients and potentials in non-relativistic effective field theory. The ingredients required up to the third order in non-relativistic perturbation theory are reviewed in [30]. Figure 10 shows the second-order (NNLO) result from [31], which exhibits a toponium resonance slightly below the nominal threshold. Note the order counting here is such that  $v \sim \alpha_s$

defines the expansion parameter. The top-quark width  $\Gamma_t/m_t \sim \alpha_{\text{EW}} \sim \alpha_s^2$  is second-order in this counting.

QCD predictions of the top-pair production cross section such as the one shown in the figure are based on the calculation of QCD correlation functions with the substitution  $E = \sqrt{s} - 2m_t \rightarrow E + i\Gamma_t$  to account for the top-quark width [21, 22]. This prescription corresponds to computing the first (resonant) term in (11) with  $\mathcal{O}_p^{(k)}$  given by the non-relativistic top-quark (axial-) vector current, and with an effective Lagrangian that accounts for the width through  $\Delta = -i\Gamma_t$  in the first bilinear term in (25) (adapted to quarks), but not in the further kinetic corrections.

The limitations of this approximation manifest themselves within the (NR)QCD calculation itself. The current correlation function  $G(E)$  exhibits an uncanceled ultraviolet divergence from an overall divergence of the form  $[\delta G(E)]_{\text{overall}} \propto \alpha_s E/\epsilon$  in dimensional regularization ( $d = 4 - 2\epsilon$ ) [32]. Since  $E$  acquires an imaginary part  $\Gamma_t \sim m_t \alpha_{\text{EW}}$ , the divergence survives in the cross section,

$$\text{Im} [\delta G(E)]_{\text{overall}} \propto m_t \times \frac{\alpha_s \alpha_{\text{EW}}}{\epsilon}, \quad (28)$$

and appears first at NNLO (since at LO,  $G(E) \sim v \sim \alpha_s$ ). A consistent calculation therefore requires that one considers the process  $e^+e^- \rightarrow W^+W^-b\bar{b}$  within unstable-particle effective theory including the effects of off-shell top quarks and processes that produce the  $W^+W^-b\bar{b}$  final state with no or only one intermediate top-quark line. The two terms of (11) can be identified with

$$\sigma_{e^+e^- \rightarrow W^+W^-b\bar{b}} = \underbrace{\sigma_{e^+e^- \rightarrow [t\bar{t}]_{\text{res}}}(\mu_W)}_{\text{pure (NR)QCD}} + \sigma_{e^+e^- \rightarrow W^+W^-b\bar{b}_{\text{nonres}}}(\mu_W). \quad (29)$$

Both terms separately have a “finite-width scale dependence” related to the uncanceled  $1/\epsilon$  poles, and only the sum is well-defined. For consistency, both terms have to be defined with the same (dimensional) regularization prescription.

While the explicit finite-width scale dependence is seen first at NNLO, the leading non-resonant contribution already appears at NLO. Somewhat surprisingly, this was realized only recently. At this order the matching coefficient of the non-resonant operator is equivalent to the dimensionally regulated  $e^+e^- \rightarrow bW^+\bar{t}$  process with  $\Gamma_t = 0$ , expanded in the hard region around

$s = 4m_t^2$ . The corresponding calculation has been performed in two independent ways [33, 34]. In [33] invariant-mass cuts  $m_t - \Delta M_t \leq M_{t,\bar{t}} \leq m_t + \Delta M_t$  on the decay products of the (anti-) top quark can be included following the method discussed above for  $W$  bosons.

It is convenient to represent the calculation of the cut two-loop diagrams contributing to  $e^+e^- \rightarrow bW^+\bar{t}$  in the form

$$\int_{\Lambda^2}^{m_t^2} dp_t^2 (m_t^2 - p_t^2)^{\frac{d-3}{2}} H_i\left(\frac{p_t^2}{m_t^2}, \frac{M_W^2}{m_t^2}\right) \quad (30)$$

leaving the integration over  $p_t^2 \equiv (p_b + p_{W^+})^2$  to the end. The lower limit depends on the invariant-mass cut and

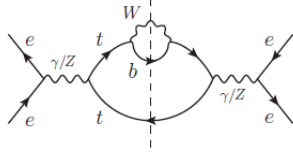


Figure 11: Hard, off-shell top diagram contribution to  $e^+e^- \rightarrow bW^+\bar{t}$ , which leads to a linear infrared divergence.

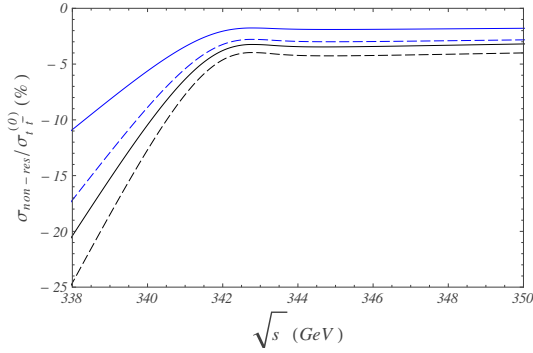


Figure 12: Relative sizes of the non-resonant corrections with respect to the  $t\bar{t}$  LO cross section in percent: NNLO singular terms  $\sigma_{\text{non-res}}^{(2)}/\sigma_{t\bar{t}}^{(0)}$  (upper blue lines) and NLO  $\sigma_{\text{non-res}}^{(1)}/\sigma_{t\bar{t}}^{(0)}$  (lower black lines). Solid (dashed) lines correspond to an invariant-mass cut  $\Delta M_t = 35$  GeV ( $\Delta M_t = 15$  GeV). Figure from [35]. Here the top pole mass  $m_t = 172$  GeV is used as input parameter.

is given by  $\Delta = M_W^2$ , when no cut is applied. The finite-width infrared divergence of the non-resonant matching coefficient that cancels the corresponding ultraviolet divergence of the non-relativistic current correlation function appears as an endpoint divergence of the integral above as  $p_t^2 \rightarrow m_t^2$  approaches the on-shell value. At NLO, the divergence arises only from the diagram shown in Figure 11. The integrand behaves as

$$H_1\left(\frac{p_t^2}{m_t^2}, \frac{M_W^2}{m_t^2}\right) \xrightarrow{p_t^2 \rightarrow m_t^2} \text{const} \times \frac{1}{(m_t^2 - p_t^2)^2}, \quad (31)$$

which leads to a divergent integral (30) in four dimensions. Dimensional regularization sets such linearly divergent integrals to finite numbers, which explains the absence of explicit  $\mu_w$  scale dependence at this order.

Similar to the case of  $W$ -boson pair production, the leading non-resonant contribution to the top-pair cross section is a nearly energy-independent, negative correction, which amounts to a few percent above the toponium peak, and to around 20% a few GeV below the peak. With an invariant-mass cut the NLO correction is shown as the lower (black) solid and dashed lines in Figure 12.

Since the largest sensitivity to the top-quark mass comes from the steep rise of the cross section below the peak, the non-resonant contributions at NLO and even NNLO are essential. The NNLO terms correspond to three-loop cut diagrams. The complete calculation has not yet been performed. However, in the presence of an invariant-mass cut satisfying  $\Gamma_t \ll \Delta M_t \ll m_t$ , the singular terms as  $m_t/\Delta M_t \rightarrow \infty$  have been extracted in two different ways [35, 36].<sup>5</sup> The calculation of [35], which starts from the non-resonant side, also confirms explicitly the cancellation of  $1/\epsilon$  finite-width divergence poles with the non-relativistic contributions. The upper set of lines (blue solid and dashed) in Figure 12, shows that the NNLO correction is only about half as large than the NLO one.

#### 4. Summary and further results

In this article I reviewed the treatment of unstable particles in perturbative quantum field theory based on the scale hierarchy  $\Gamma \ll M$ . Once scale separation is taken as the guiding principle, and an effective field theory is constructed, gauge-invariance and the consistency of the all-order resummation is automatic. The effective theory describes the scattering processes that leave the resonance close to its complex mass shell. Some aspects are therefore closely related to other effective theories that describe heavy particles close to their mass-shell. The concrete applications considered so far can be described by the master formula (11), which captures resonant production and decay, as well as all non-resonant “background” processes.

The effective theory approach appears most fruitful, when it is applied to inclusive quantities, where it leads to particularly simple, even completely analytic results; to processes that require other resummations on top of the self-energy of the unstable particle; and to processes where high precision is required, beyond NLO accuracy, for which automated tools are not yet available. The line-shape and pair production near threshold discussed here are examples of such situations.

As with other effective theories it is more difficult to predict differential distributions, unless the scales associated with the observable can be assigned a unique scaling with respect to the small parameters that define the EFT expansion. To circumvent this problem, a hybrid approach has been followed in [38, 39], applicable to NLO calculations, in which the simplifica-

<sup>5</sup>Further, the leading term in an expansion in the parameter  $\rho = 1 - M_W/m_t$  has been obtained in [34] and [37], with different results.

tions provided by the EFT are used in the virtual corrections (which have tree kinematics), while real emission is computed in the full theory with the complex-mass prescription. A fully differential calculation has been done recently for the mixed  $\mathcal{O}(\alpha_{\text{em}}\alpha_s)$  corrections to Drell-Yan production [40] employing a mixture of diagrammatic and EFT-inspired techniques.

### Acknowledgements

This review summarizes work performed within and supported by the DFG Sonderforschungsbereich/Transregio 9 “Computational Theoretical Particle Physics”. I wish to thank my collaborators on this project, in particular P. Falgari, B. Jantzen, P. Ruiz-Femenia, Ch. Schwinn, A. Signer and G. Zanderighi.

### References

- [1] M. J. G. Veltman, Unitarity and causality in a renormalizable field theory with unstable particles, *Physica* 29 (1963) 186–207.
- [2] M. Beneke, A. P. Chapovsky, A. Signer, G. Zanderighi, Effective theory approach to unstable particle production, *Phys. Rev. Lett.* 93 (2004) 011602. [arXiv:hep-ph/0312331](#).
- [3] M. Beneke, A. P. Chapovsky, A. Signer, G. Zanderighi, Effective theory calculation of resonant high-energy scattering, *Nucl. Phys. B* 686 (2004) 205–247. [arXiv:hep-ph/0401002](#).
- [4] R. G. Stuart, Gauge invariance, analyticity and physical observables at the  $Z^0$  resonance, *Phys. Lett. B* 262 (1991) 113–119.
- [5] A. Aeppli, G. J. van Oldenborgh, D. Wyler, Unstable particles in one loop calculations, *Nucl. Phys. B* 428 (1994) 126–146. [arXiv:hep-ph/9312212](#).
- [6] W. Beenakker, F. A. Berends, A. P. Chapovsky, Radiative corrections to pair production of unstable particles: Results for  $e^+e^- \rightarrow 4$  fermions, *Nucl. Phys. B* 548 (1999) 3–59. [arXiv:hep-ph/9811481](#).
- [7] A. Denner, S. Dittmaier, M. Roth, D. Wackeroth,  $\mathcal{O}(\alpha)$  corrections to  $e^+e^- \rightarrow W^+W^- \rightarrow 4$  fermions ( $+\gamma$ ): First numerical results from racoonww, *Phys. Lett. B* 475 (2000) 127–134. [arXiv:hep-ph/9912261](#).
- [8] A. P. Chapovsky, V. A. Khoze, A. Signer, W. J. Stirling, Non-factorizable corrections and effective field theories, *Nucl. Phys. B* 621 (2002) 257–302. [arXiv:hep-ph/0108190](#).
- [9] R. Stuart, Pitfalls of radiative corrections near a resonance, in: *Z0 physics, Proceedings of the 25th Rencontre de Moriond, Lepton Session, Les Arcs, France, March 4–11, 1990*, J. Tran Thanh Van (ed.).
- [10] A. Denner, S. Dittmaier, M. Roth, L. H. Wieders, Electroweak corrections to charged-current  $e^+e^- \rightarrow 4$  fermion processes: Technical details and further results, *Nucl. Phys. B* 724 (2005) 247–294. [arXiv:hep-ph/0505042](#).
- [11] T. Bauer, J. Gegelia, G. Japaridze, S. Scherer, Complex-mass scheme and perturbative unitarity, *Int.J.Mod.Phys. A* 27 (2012) 1250178. [arXiv:1211.1684](#).
- [12] A. Denner, J.-N. Lang, The Complex-Mass Scheme and Unitarity in perturbative Quantum Field Theory, [arXiv:1406.6280](#).
- [13] D. Y. Bardin, M. S. Bilenky, W. Beenakker, F. A. Berends, W. van Neerven, et al., Z line-shape, in: *Proceedings of “Z physics at LEP 1”*, Geneva 1989, p. 89–127, CERN-TH-5468-89.
- [14] M. Beneke, V. A. Smirnov, Asymptotic expansion of Feynman integrals near threshold, *Nucl. Phys. B* 522 (1998) 321–344. [arXiv:hep-ph/9711391](#).
- [15] E. Eichten, B. R. Hill, An Effective Field Theory for the Calculation of Matrix Elements Involving Heavy Quarks, *Phys. Lett. B* 234 (1990) 511.
- [16] C. W. Bauer, S. Fleming, D. Pirjol, I. W. Stewart, An effective field theory for collinear and soft gluons: Heavy to light decays, *Phys. Rev. D* 63 (2001) 114020. [arXiv:hep-ph/0011336](#).
- [17] C. W. Bauer, D. Pirjol, I. W. Stewart, Soft-collinear factorization in effective field theory, *Phys. Rev. D* 65 (2002) 054022. [arXiv:hep-ph/0109045](#).
- [18] M. Beneke, A. P. Chapovsky, M. Diehl, T. Feldmann, Soft-collinear effective theory and heavy-to-light currents beyond leading power, *Nucl. Phys. B* 643 (2002) 431–476. [arXiv:hep-ph/0206152](#).
- [19] M. Beneke, T. Feldmann, Multipole expanded soft collinear effective theory with nonAbelian gauge symmetry, *Phys. Lett. B* 553 (2003) 267–276. [arXiv:hep-ph/0211358](#).
- [20] V. S. Fadin, V. A. Khoze, A. D. Martin, W. J. Stirling, Higher order Coulomb corrections to the threshold  $e^+e^- \rightarrow W^+W^-$  cross-section, *Phys. Lett. B* 363 (1995) 112–117. [arXiv:hep-ph/9507422](#).
- [21] V. S. Fadin, V. A. Khoze, Threshold behavior of heavy top production in  $e^+e^-$  collisions, *JETP Lett.* 46 (1987) 525–529.
- [22] V. S. Fadin, V. A. Khoze, Production of a pair of heavy quarks in  $e^+e^-$  annihilation in the threshold region, *Sov. J. Nucl. Phys.* 48 (1988) 309–313.
- [23] M. Beneke, P. Falgari, C. Schwinn, A. Signer, G. Zanderighi, Four-fermion production near the W pair production threshold, *Nucl. Phys. B* 792 (2008) 89–135. [arXiv:0707.0773](#).
- [24] S. Actis, M. Beneke, P. Falgari, C. Schwinn, Dominant NNLO corrections to four-fermion production near the W-pair production threshold, *Nucl. Phys. B* 807 (2009) 1–32. [arXiv:0807.0102](#).
- [25] A. Pineda, J. Soto, Potential NRQED: The positronium case, *Phys. Rev. D* 59 (1999) 016005. [arXiv:hep-ph/9805424](#).
- [26] W. Kilian, T. Ohl, J. Reuter, WHIZARD: Simulating Multi-Particle Processes at LHC and ILC, *Eur. Phys. J. C* 71 (2011) 1742. [arXiv:0708.4233](#).
- [27] A. Pukhov, et al., CompHEP: A package for evaluation of Feynman diagrams and integration over multi-particle phase space. User’s manual for version 33, [arXiv:hep-ph/9908288](#).
- [28] A. Denner, S. Dittmaier, M. Roth, L. H. Wieders, Complete electroweak  $\mathcal{O}(\alpha)$  corrections to charged-current  $e^+e^- \rightarrow 4$  fermion processes, *Phys. Lett. B* 612 (2005) 223–232. [arXiv:hep-ph/0502063](#).
- [29] M. Beneke, A quark mass definition adequate for threshold problems, *Phys. Lett. B* 434 (1998) 115–125. [arXiv:hep-ph/9804241](#).
- [30] M. Beneke, Y. Kiyo, K. Schuller, Third-order correction to top-quark pair production near threshold I. Effective theory set-up and matching coefficients, [arXiv:1312.4791](#).
- [31] M. Beneke, A. Signer, V. A. Smirnov, Top quark production near threshold and the top quark mass, *Phys. Lett. B* 454 (1999) 137–146. [arXiv:hep-ph/9903260](#).
- [32] M. Beneke, Y. Kiyo, Ultrasoft contribution to heavy-quark pair production near threshold, [arXiv:0804.4004](#).
- [33] M. Beneke, B. Jantzen, P. Ruiz-Femenia, Electroweak non-resonant NLO corrections to  $e^+e^- \rightarrow W^+W^-b\bar{b}$  in the  $t\bar{t}$  resonance region, *Nucl. Phys. B* 840 (2010) 186–213. [arXiv:1004.2188](#).
- [34] A. A. Penin, J. H. Piclum, Threshold production of unstable top, *JHEP* 1201 (2012) 034. [arXiv:1110.1970](#).
- [35] B. Jantzen, P. Ruiz-Femenia, Next-to-next-to-leading order non-

- resonant corrections to threshold top-pair production from  $e^+e^-$  collisions: Endpoint-singular terms, *Phys.Rev. D*88 (5) (2013) 054011. [arXiv:1307.4337](#).
- [36] A. H. Hoang, C. J. Reisser, P. Ruiz-Femenia, Phase Space Matching and Finite Lifetime Effects for Top-Pair Production Close to Threshold, *Phys. Rev. D*82 (2010) 014005. [arXiv:1002.3223](#).
- [37] P. Ruiz-Femenia, First estimate of the NNLO nonresonant corrections to top-antitop threshold production at lepton colliders, *Phys.Rev. D*89 (9) (2014) 097501. [arXiv:1402.1123](#).
- [38] P. Falgari, P. Mellor, A. Signer, Production-decay interferences at NLO in QCD for  $t$ -channel single-top production, *Phys.Rev. D*82 (2010) 054028. [arXiv:1007.0893](#).
- [39] P. Falgari, A. Papanastasiou, A. Signer, Finite-width effects in unstable-particle production at hadron colliders, *JHEP* 1305 (2013) 156. [arXiv:1303.5299](#).
- [40] S. Dittmaier, A. Huss, C. Schwinn, Mixed QCD-electroweak  $O(\alpha_s\alpha)$  corrections to Drell-Yan processes in the resonance region: pole approximation and non-factorizable corrections, *Nucl.Phys. B*885 (2014) 318–372. [arXiv:1403.3216](#).